

## Supporting information

# Ordered Mesoporous SnO<sub>2</sub> Based Photoanodes for High Performance Dye-Sensitized Solar Cells

Easwaramoorthi Ramasamy and Jinwoo Lee\*

Department of Chemical Engineering, School of Environmental Science and Engineering,  
Pohang University of Science and Technology (POSTECH), Pohang, Korea

Email: jinwoo03@postech.ac.kr

### *Synthesis of KIT-6 silica*

Mesoporous KIT-6 silica was synthesized by following published procedures.<sup>1</sup> Nitrogen sorption isotherm in Figure.S1 indicates the mesoporous structure of the KIT-6 silica with pore size distribution centered at 8 nm. The Brunauer-Emmett-Teller (BET) surface area and pore volume of KIT-6 silica are 874 m<sup>2</sup>/g and 1.14 cm<sup>3</sup>/g, respectively.

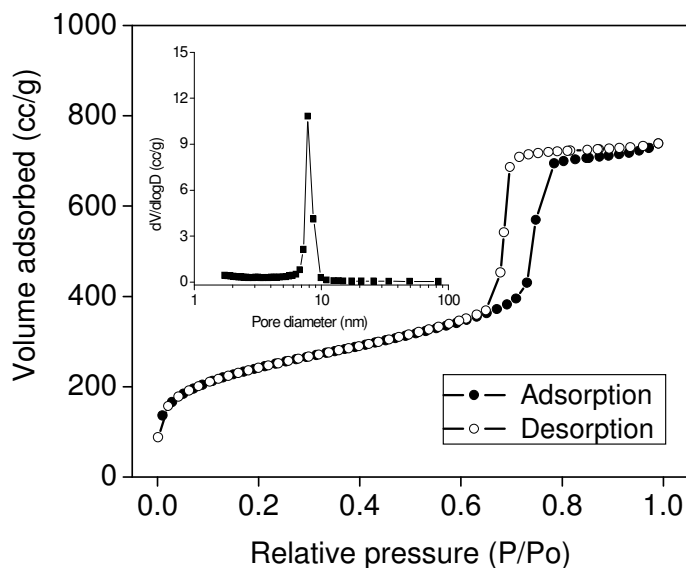


**Figure S1.** N<sub>2</sub> sorption isotherm and the corresponding BJH pore size distribution (inset) of KIT-6 silica obtained from the adsorption isotherm.

### *Synthesis of ordered mesoporous SnO<sub>2</sub>*

Ordered mesoporous SnO<sub>2</sub> (here after, meso-SnO<sub>2</sub>) was synthesized by using SnCl<sub>2</sub>·2H<sub>2</sub>O as a tin precursor and KIT-6 silica as a hard template. Figure S2 schematically shows the possible scenario during the nanocasting process. The impregnation of SnCl<sub>2</sub>·2H<sub>2</sub>O in both chiral channels resulted in meso-SnO<sub>2</sub> with 3 nm pores while filling in either one of two chiral channel leads to ~20 nm wide pores.<sup>2,3</sup>

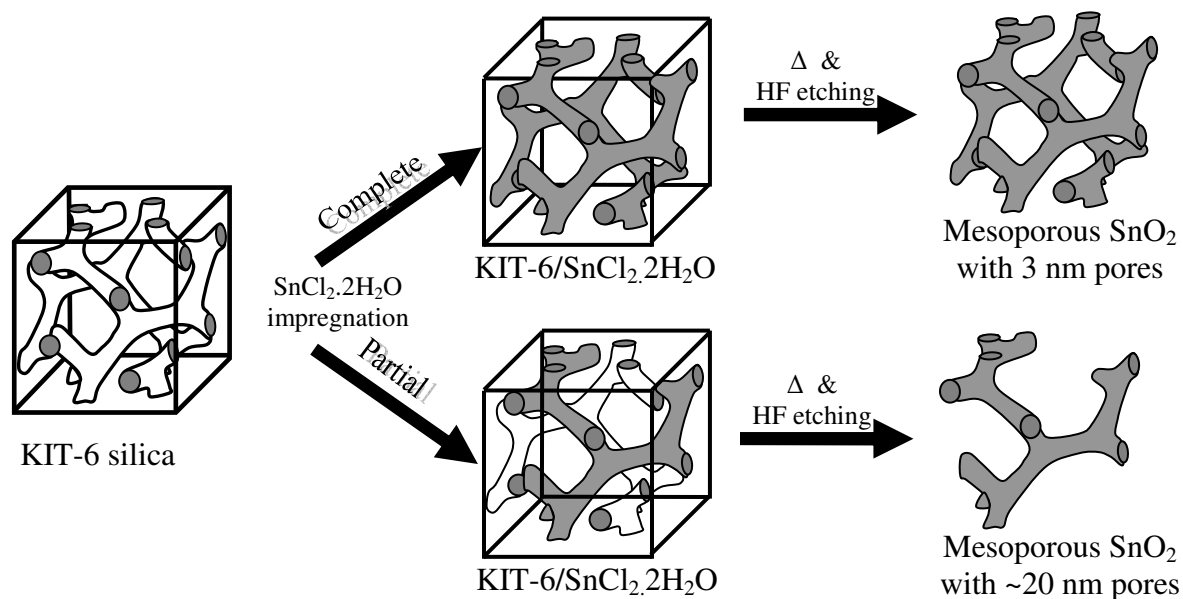


**Figure S2.** Schematic representation of ordered mesoporous SnO<sub>2</sub> with bimodal pores, replicated from KIT-6 silica template.

### *SEM and TEM images*

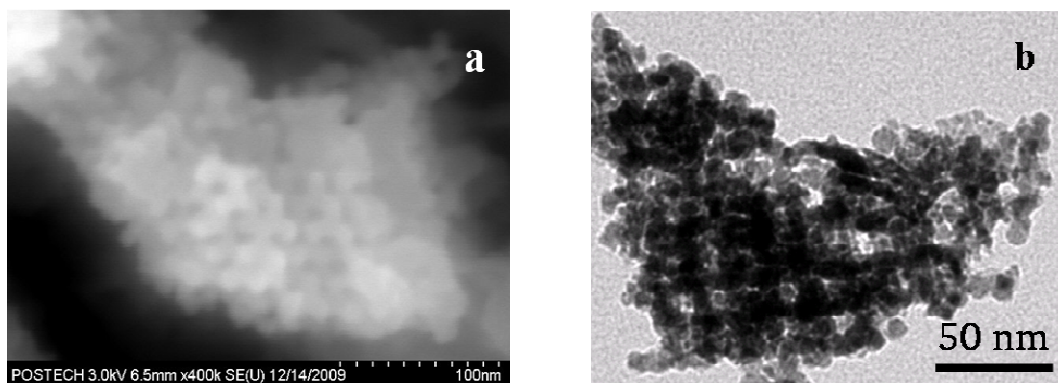


**Figure S3.** (a) SEM , and (b) TEM images of meso-SnO<sub>2</sub> powders. These two images show the large size pores which are generated by the impregnation of precursor in either one of two chiral channels.

### *Small angle X-ray scattering pattern*

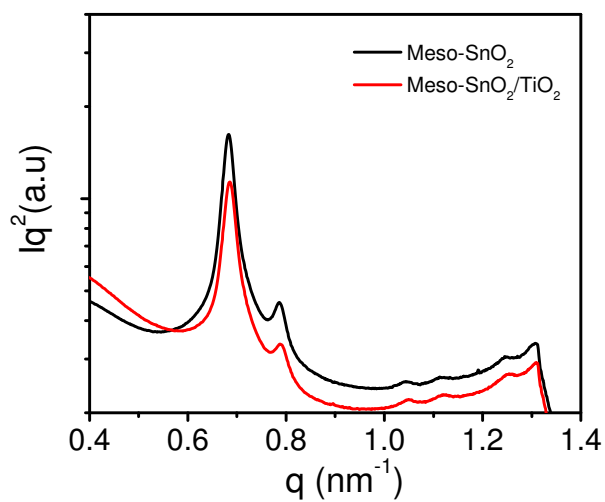


**Figure S4.** Small angle X-ray scattering (SAXS) pattern of meso-SnO<sub>2</sub> and meso-SnO<sub>2</sub>/TiO<sub>2</sub> core-shell powders.

*SEM cross section view of photoanodes*

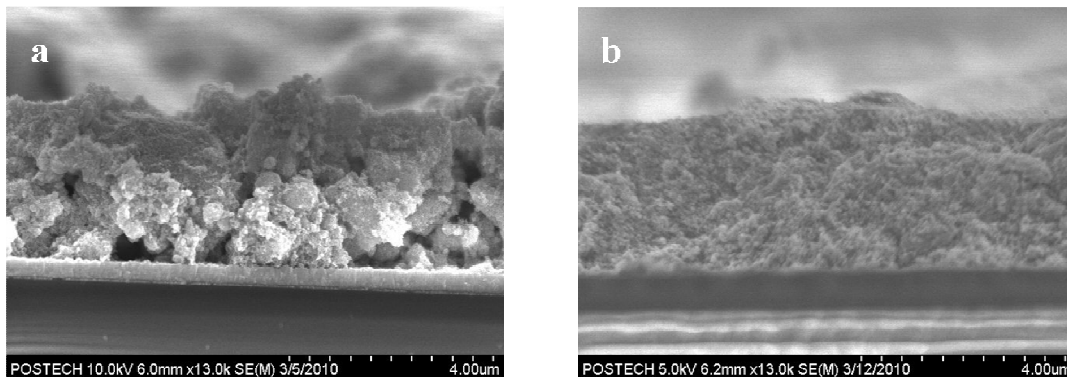


**Figure S5.** Cross-sectional SEM images of (a) Meso-SnO<sub>2</sub>, and (b) Nano-SnO<sub>2</sub> photoanode.

*Photoinduced degradation mechanism in DSSCs*

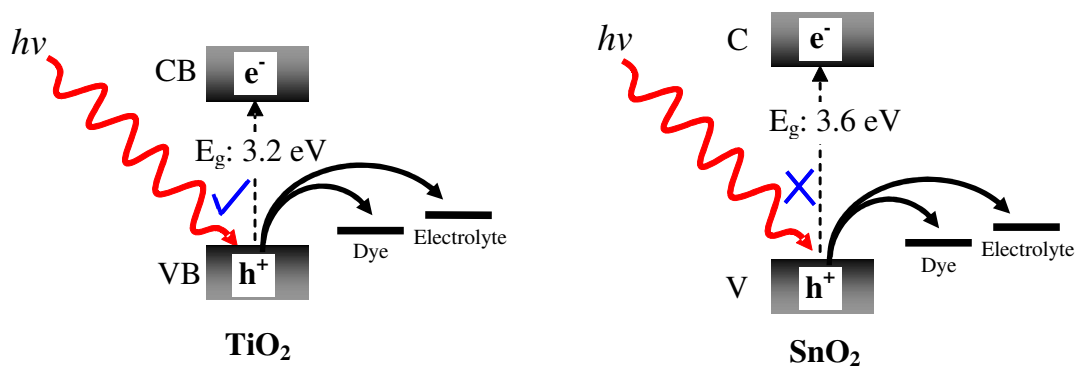


**Figure S6.** Schematic of photoinduced degradation mechanism in DSSCs. Incident photon with sufficient energy liberates electron from the valence band of TiO<sub>2</sub> and thereby creating holes (h<sup>+</sup>). These holes are likely to i) oxidize the dye molecules and degrade the TiO<sub>2</sub> /dye interface, ii) irreversibly oxidize the I<sup>-</sup> to I<sub>3</sub><sup>-</sup> and leads to the unrecoverable loss of I<sub>3</sub><sup>-</sup> ions in the redox electrolyte.<sup>4,5</sup> These both outcomes are notably affect the overall stability of DSSCs. To prevent the photo-induced degradation in TiO<sub>2</sub>

photoanode DSSCs, UV cut-off filter is typically placed on the front side of the device and accelerated aging tests are carried out.<sup>6</sup> On the other hand, larger band gap of SnO<sub>2</sub> would create fewer oxidative holes in the valence band thereby minimize the dye degradation and improve the long-term stability of DSSCs.

***References:***

1. Kim, T. W.; Kleitz, F.; Paul, B.; Ryoo, R. *J. Am. Chem. Soc.* **2005**, *127*, 7601.
2. Shin, H. J.; Ryoo, R.; Liu, Z.; Terasaki, O. *J. Am. Chem. Soc.* **2001**, *123*, 1246.
3. Jiao, F.; Hill, A. H.; Harrison, A.; Berko, A.; Chadwick, A.V.; Bruce, P. G. *J. Am. Chem. Soc.* **2008**, *130*, 5262.
4. Hinsch, A.; Kroon, J. M.; Kern, R.; Uhlendorf, I.; Holzbock, J.; Meyer, A.; Ferber, J. *Prog. Photovolt. Res. Appl.* **2001**, *9*, 425.
5. Kay, A.; Grätzel, M. *Chem. Mater.* **2002**, *14*, 2930.
6. Wang, P.; Zakeeruddin, S.M.; Moser, J.E.; Nazeeruddin, M.K.; Sekiguchi, T.; Grätzel, M. *Nat. Mater.* **2003**, *2*, 402.